Free Radical Research, August 2006; 40(8): 875–884

informa
healthcare

4-Hydroxy-2-nonenal upregulates endogenous antioxidants and phase 2 enzymes in rat H9c2 myocardiac cells: Protection against overt oxidative and electrophilic injury

HONG ZHU, LI ZHANG, XIAOQING XI, JAY L. ZWEIER & YUNBO LI

Department of Internal Medicine and Division of Cardiovascular Medicine, Davis Heart and Lung Research Institute, The Ohio State University College of Medicine and Public Health, 473 West 12th Avenue, Columbus, OH 43210, USA

Accepted by Professor E. Niki

(Received 11 March 2006; in revised form 18 April 2006)

Abstract
This study was undertaken to determine if 4-hydroxy-2-nonenal (HNE) could upregulate antioxidants and phase 2 enzymes in rat H9c2 myocardiac cells, and if the upregulated defenses led to cytoprotection against oxidative and electrophilic injury. Incubation of H9c2 cells with HNE at noncytotoxic concentrations resulted in significant induction of cellular catalase, glutathione (GSH), GSH S-transferase (GST), and NAD(P)H:quinone oxidoreductase 1 (NQO1), as determined by enzyme activity and/or protein expression. HNE treatment caused increased mRNA expression of catalase, γ-glutamylcysteine ligase, GST-A1, and NQO1. Pretreatment of H9c2 cells with HNE led to significant protection against cytotoxicity induced by reactive oxygen and nitrogen species. HNE-pretreated cells also exhibited increased resistance to injury elicited by subsequent cytotoxic concentrations of HNE. Taken together, this study demonstrates that several antioxidants and phase 2 enzymes in H9c2 cells are upregulated by HNE and that the increased defenses afford protection against overt oxidative and electrophilic cardiac cell injury.

Keywords: *4-Hydroxy-2-nonenal, cardiac cells, antioxidants, phase 2 enzymes, cytotoxicity*

Abbreviations: *CDNB, 1-chloro-2,4-dinitrobenzene; DCFH, 2,7-dichlorodihydrofluorescein; DCIP, 2,6-dichloroindophenol; FBS, fetal bovine serum; GCL, γ-glutamylcysteine ligase; GPx, glutathione peroxidase; GR, glutathione reductase; GSH, reduced glutathione; GSSG, oxidized form of glutathione; GST, glutathione S-transferase; HNE, 4-hydroxy-2-nonenal; LDH, lactate dehydrogenase; MTT, 3-[4,5-dimethylthiazol-2-yl]-2,5-diphenyltetrazolium bromide; NQO1, NAD(P)H:quinone oxidoreductase-1; PBS, phosphate buffered saline; RNS, reactive nitrogen species; ROS, reactive oxygen species; SIN-1, 3-morpholinosydnonimine; SOD, superoxide dismutase*

Introduction

The α, β-unsaturated aldehyde 4-hydroxy-2-nonenal (HNE) is formed by the reaction of reactive oxygen or nitrogen species (ROS/RNS) with arachidonic acid in cellular membranes during inflammation and other pathophysiological conditions [1]. HNE is present in the free form at 0.3–0.7 μM in human plasma in healthy individuals and can increase 10 times or more during oxidative stress *in vivo* [2,3]. It is estimated the levels of HNE in local tissues or cells under oxidative stress conditions can reach up to 20 μM [2].

HNE is a potent electrophile, and can react in Michael additions across its carbon–carbon double bond with various cellular components, including

Correspondence: Y. Li, Davis Heart and Lung Research Institute, The Ohio State University College of Medicine and Public Health, Room 012C, 473 West 12th Avenue, Columbus, OH 43210, USA. Tel: 1 614 292 4811. Fax: 1 614 247 7799. E-mail: yunbo.li@osumc.edu

ISSN 1071-5762 print/ISSN 1029-2470 online © 2006 Informa UK Ltd
DOI: 10.1080/10715760600778694

protein and nucleic acids [1]. Due to its high reactivity and ubiquitous occurrence in biological systems, HNE has been implicated in a number of pathophysiological processes, including neurodegeneration, aging, atherosclerosis and myocardial ischemia-reperfusion injury [1,4]. HNE at micromolar concentrations is able to elicit cell dysfunction and cytotoxicity in a variety of cell types [1]. We previously observed that HNE at concentrations greater than 10 μM induced significant cytotoxicity in cultured cardiomyocytes and vascular smooth muscle cells [5,6]. While a number of cellular factors are known to participate in the metabolism of HNE in cells, conjugation of HNE with GSH is found to be the principal pathway leading to its detoxification [5–7]. Interestingly, it has been repeatedly observed that γ-glutamylcysteine ligase (GCL), the rate-limiting enzyme in GSH biosynthesis, can be induced by HNE, particularly at noncytotoxic concentrations [8]. This suggests that induction of GCL/GSH and possibly other cytoprotective factors by HNE may be an adaptive response leading to detoxification of itself as well as other ROS/RNS.

Although induction of GCL activity and GSH synthesis by HNE and the underlying signaling mechanisms have been investigated [8], studies on the ability of HNE to upregulate other cellular antioxidants and phase 2 enzymes in cardiac cells are currently lacking. In this study, using rat myocardiac H9c2 cells, we have investigated the concentration-dependent inducibility of a series of endogenous antioxidants and phase 2 enzymes by HNE at noncytotoxic concentrations, and the resultant cytoprotective effects on overt oxidative and electrophilic stress. Our results demonstrate that several antioxidants and phase 2 enzymes, including catalase, GSH/GCL, GSH S-transferase (GST) and NAD(P)H:quinone oxidoreductase 1 (NQO1) can be upregulated by HNE, and that the upregulated cellular defenses are accompanied by increased resistance to cell injury elicited by ROS/RNS as well as exposure to the subsequent cytotoxic concentrations of HNE itself.

Materials and methods

Materials

HNE was from Cayman Chemical (Ann Arbor, MI, USA). Dulbecco's modified Eagle's medium (DMEM), penicillin, streptomycin, and fetal bovine serum (FBS) were from Gibco-Invitrogen (Carlsbad, CA, USA). All other chemicals and reagents were from Sigma Chemical (St Louis, MO, USA).

Cell culture and preparation of cell extract

H9c2 cells (ATCC, Manassas, VA, USA) were cultured in DMEM supplemented with 10% FBS, 100 U/ml of penicillin, and 100 μg/ml of streptomycin in tissue culture flasks at 37°C in a humidified atmosphere of 5% CO_2. The cells were fed every 2–3 days, and subcultured once they reached 70–80% confluence. Experimental treatments were applied to cells at an initial confluence of ~80%. To make cell extract for measurement of antioxidants and phase 2 enzymes, H9c2 cells were collected and resuspended in ice-cold 50 mM potassium phosphate buffer, pH 7.4, containing 2 mM EDTA and 0.1% Triton X-100. The cells were sonicated, followed by centrifugation at 13,000*g* for 10 min at 4°C. The resulting supernatants were collected and the protein concentrations were quantified with Bio-Rad protein assay dye (Hercules, CA, USA).

Superoxide dismutase (SOD) assay

Total cellular SOD activity was determined by the method of Spitz and Oberley [9] with slight modifications, as described before [10]. The sample total SOD activity was calculated using a concurrently run SOD (Sigma Chemical) standard curve, and expressed as units per mg of cellular protein.

Catalase assay

The method of Aebi [11] was used to measure cellular catalase activity, which was expressed as μmol of H_2O_2 consumed per min per mg of cellular protein.

GSH assay

Cellular GSH content was measured according to the fluorometric assay described previously, which is specific for GSH measurement at pH 8.0 [10]. Cellular GSH content was calculated using a concurrently run GSH (Sigma Chemical) standard curve, and expressed as nmol of GSH per mg of cellular protein.

Glutathione reductase (GR) assay

Cellular GR activity was measured according to the method of Wheeler et al. [12] with modifications, as described previously [10]. GR activity was calculated using the extinction coefficient of 6.22 $mM^{-1}cm^{-1}$, and expressed as nmol of NADPH consumed per min per mg of cellular protein.

GSH peroxidase (GPx) assay

Cellular GPx activity was measured by the method of Flohe and Gunzler [13] with slight modifications, as described before [10]. H_2O_2 was used as the substrate, and GPx activity was calculated using the extinction coefficient of 6.22 $mM^{-1}cm^{-1}$, and expressed as nmol

of NADPH consumed per min per mg of cellular protein.

GST assay

1-Chloro-2,3-dinitrobenzene (CDNB) was used as the substrate for measuring GST activity. GST activity was calculated using the extinction coefficient of 9.6 $mM^{-1}cm^{-1}$, and expressed as nmol of CDNB–GSH conjugate formed per min per mg of cellular protein [10].

NQO1 assay

Cellular NQO1 activity was determined using dichloroindophenol (DCIP) as the 2-electron acceptor, as described before [10]. The dicumarol-inhibitable NQO1 activity was calculated using the extinction coefficient of 21.0 $mM^{-1}cm^{-1}$, and expressed as nmol of DCIP reduced per min per mg of cellular protein.

RNA isolation and RT-PCR detection of mRNA levels

Total RNA from H9c2 cells was extracted using Trizol reagent (Invitrogen, Carlsbad, CA, USA). cDNA synthesis and subsequent PCR reactions were performed using Superscript II One-Step system (Invitrogen). The cycling conditions for RT-PCR were the following: 50°C for 30 min (reverse transcription), 94°C for 2 min (pre-denaturation), followed by 25 cycles of PCR amplification process including denaturing at 94°C for 15 s, annealing at 57°C for 30 s, and extension at 72°C for 45 s, and by one cycle of final extension at 72°C for 10 min. The sequences of the PCR primers are shown in Table I. PCR products were separated by agarose gel electrophoresis, and stained with ethidium bromide. The gels were then analyzed under ultraviolet light using an Alpha Innotech Imaging system (San Leandro, CA, USA). In this study, a standard curve for each of the antioxidant/phase 2 enzyme mRNAs using various amounts of total RNA was included in each assay so as to reliably estimate changes in mRNA levels. We and others have previously demonstrated the quantitative capacity of RT-PCR in conjunction with RNA standard curve in analysis of mRNA levels [14,15].

Immunoblot analysis

The immunoblot procedures described before [14] were followed to detect protein expression. Briefly, cells were lysed by sonication followed by centrifugation to yield the supernatant samples. Equal amounts of protein from each of the samples were resolved by SDS-PAGE on 10% gels, transferred electrophoretically to a nitrocellulose membrane (Amersham Biosciences, Piscataway, NJ, USA). The membrane was blocked with 5% non-fat dried milk in TTBS buffer at room temperature for 1.5 h. The membrane was then incubated with primary antibodies (anti-GCL, 1:500; anti-NQO1, 1:500; anti-β-actin, 1:2000) (Santa Cruz Biotech, CA, USA) overnight at 4°C, followed by incubation with horseradish peroxidase-labeled secondary antibody (Santa Cruz Biotech) at room temperature for another 1.5 h. The membrane was visualized using an enhanced chemiluminescence system (Amersham Biosciences) and blots were quantified by Alpha Innotech Imaging system.

Table I. Oligonucleotide sequences for RT-PCR analysis of gene expression of antioxidants and phase 2 enzymes.

Enzymes	Primers	
Catalase	Sense	5′-GACATGGTCTGGGACTTCTG-3′
	Antisense	5′-GTAGGGACAGTTCACAGGTA-3′
GCL-C	Sense	5′-CCTTCTGGCACAGCACGTTG-3′
	Antisense	5′-TAAGACGGCATCTCGCTCCT-3′
GST-A1	Sense	5′-GAAGCCAGTCCTTCACTACT-3′
	Antisense	5′-CAGCTCTTCCACATGGTAGA-3′
NQO1	Sense	5′-CCATTCTGAAAGGCTGGTTTG-3′
	Antisense	5′-CTAGCTTTGATCTGGTTGTC-3′
β-Actin	Sense	5′-GACAACGGCTCCGGCATGT-3′
	Antisense	5′-GCAACATAGCACAGCTTCT-3′

Cell viability assays

Cell viability was determined by both 3-[4,5-dimethylthiazol-2-yl]-2,5-diphenyltetrazolium (MTT) reduction assay and lactate dehydrogenase (LDH) release assay. The procedures described previously [14] were followed to detect cell viability by MTT reduction assay. The method described by Li et al. [5] was used with slight modifications to measure LDH activity directly in the media collected from cell cultures. Briefly, to an assay cuvette, 250 μl of culture medium, 190 μl of phosphate-buffered saline (PBS) and 30 μl of sodium pyruvate (5.5 mM prepared in PBS) were added. 30 μl of NADH (4 mM prepared in PBS) was then added to start the reaction. The LDH-catalyzed NADH consumption was monitored at 340 nm, 25°C for 5 min. LDH activity was calculated using the extinction coefficient of 6.22 $mM^{-1}cm^{-1}$, and expressed as nmoles of NADH consumed per min per ml of culture medium.

2′,7′-Dichlorodihydrofluorescein (DCFH) assay

Fluorescent measurement of DCFH oxidation was carried out to determine intracellular ROS levels in H9c2 cells according to the procedures described previously by Cao et al. [16].

Statistical analysis

All data are expressed as means ± SEM from at least three separate experiments. Differences between mean values of multiple groups were analyzed by one-way analysis of variance (ANOVA) followed by Student–Newman-Keuls test. Differences between two groups were analysed by Student *t*-test. Results were considered statistically significant when $p < 0.05$.

Results

Concentration-dependent induction of cytotoxicity by HNE

To set the stage for the subsequent experiments, we first determined the concentration-dependent induction of cytotoxicity by HNE in H9c2 cells. As shown in Figure 1, incubation of H9c2 with 2.5–10 μM HNE for 24 h did not cause any significant cytotoxicity as assessed by both MTT reduction and LDH release. However, significant cytotoxicity ensured after exposure of the cells to 15–35 μM HNE for 24 h. The induction of cytotoxicity by HNE showed a concentration-dependent fashion (Figure 1). We thus selected the non-cytotoxic concentrations (2.5–10 μM) of HNE to investigate the inducibility of cellular antioxidants and phase 2 enzymes in H9c2 cells.

Inducibility of SOD and catalase by HNE at noncytotoxic concentrations

Incubation of H9c2 cells with 2.5–10 μM HNE for 24 h did not lead to any significant changes in SOD activity (Figure 2(A)). In contrast, the same HNE treatment resulted in significant induction of catalase activity (Figure 2(B)). RT-PCR analysis showed that the level of catalase mRNA was significantly increased at 6 h after incubation of H9c2 cells with 10 μM HNE; a 4.5- and 3-fold induction of catalase mRNA was observed at 15 and 24 h, respectively (Figure 3(B)). The linear PCR amplification of the catalase mRNA

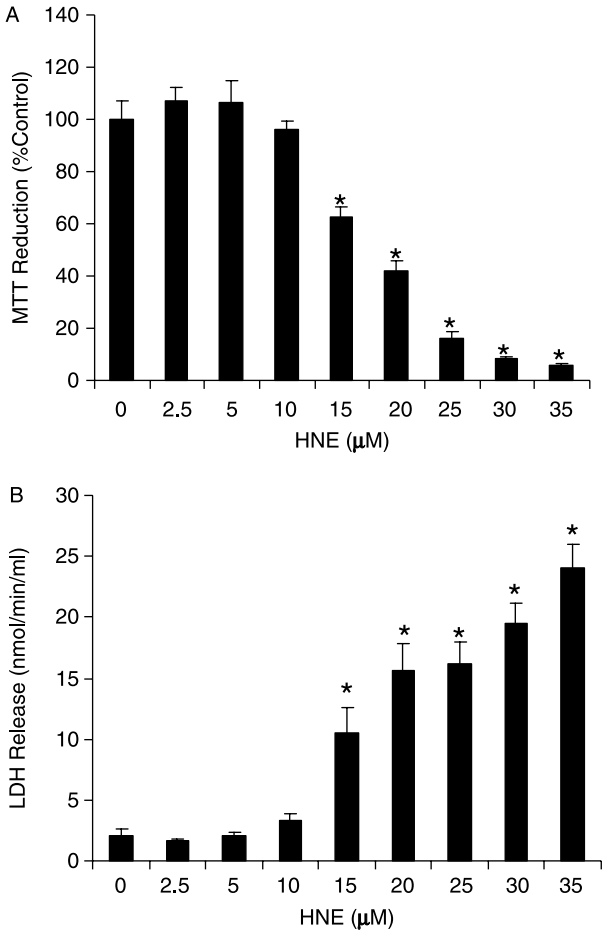

Figure 1. Concentration-dependent induction of cytotoxicity by HNE in H9c2 cells. Cells were incubated with the indicated concentrations of HNE for 24 h, followed by detection of cytotoxicity by MTT reduction (A) and LDH release (B). Values represent means ± SEM ($n = 4$). *, Significantly different from "0 μM HNE" at $p < 0.05$.

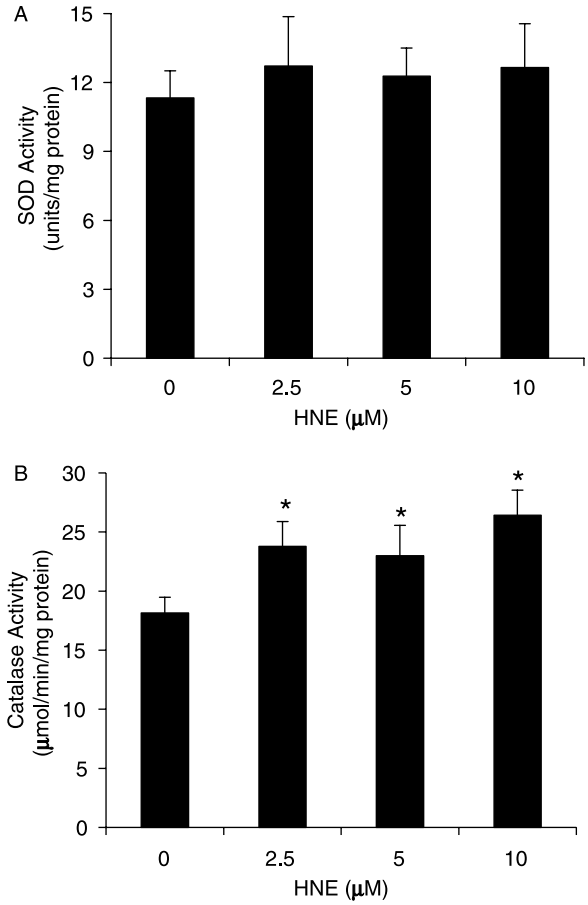

Figure 2. Effects of HNE treatment on SOD (A) and catalase (B) activities in H9c2 cells. Cells were incubated with the indicated concentrations of HNE for 24 h, followed by measurement of SOD and catalase activities. Values represent means ± SEM ($n = 4$). *, Significantly different from "0 μM HNE" at $p < 0.05$.

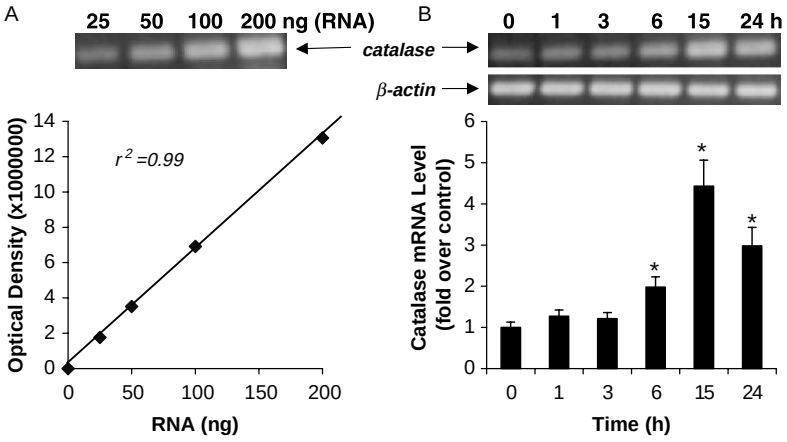

Figure 3. Standard curve for quantification of catalase mRNA levels (A) and time-dependent induction of catalase mRNA expression by HNE (B) in H9c2 cells. In (A), representative gel picture and line graph showing the linear amplification of the PCR product derived from the indicated amounts of total RNA. In (B), top panels are representative gel pictures showing the mRNA expression of catalase and β-actin at the indicated time points after treatment of H9c2 cells with 10 μM HNE; low panel shows quantitative analysis of the catalase mRNA expression. Values in (B) represent means ± SEM ($n = 3$). *, Significantly different from 0 h at $p < 0.05$.

as shown in Figure 3(A) was in line with our previous report on the quantitative capacity of RT-PCR in detection of mRNA levels [14].

Inducibility of GSH, GR and GPx by HNE at noncytotoxic concentrations

A significant concentration-dependent induction of cellular GSH was observed after incubation of H9c2 cells with 2.5–10 μM HNE for 24 h; a nearly 2-fold elevation of GSH level was seen with 10 μM HNE (Figure 4(A)). Neither GR nor GPx activity was elevated by the same HNE treatment (Figure 4(B),(C)). However, a slight, but significant decrease in GPx activity was observed in cells treated with 10 μM HNE (Figure 4(C)). Since a nearly 2-fold induction of GSH was caused by 10 μM HNE, we next examined the induction of the GCL protein as well as the mRNA expression of GCL-catalytic subunit (GCL-C). As shown in Figure 5(A), induction of GCL protein expression by HNE (2.5–10 μM) exhibited a concentration-dependent manner, which was similar to that observed with GSH induction (Figure 4(A)). Treatment of cells with 10 μM HNE also led to a time-dependent induction of GCL-C mRNA expression; a >2-fold induction of GCL-C mRNA expression was observed at 3–15 h after HNE treatment (Figure 5(B)). In data not shown, the mRNA expression of GCL regulatory subunit was also remarkably induced by 10 μM HNE.

Inducibility of GST and NQO1 by HNE at non-cytotoxic concentrations

Both GST and NQO1 activities were significantly increased in H9c2 cells after incubation with 2.5–10 μM HNE for 24 h in a concentration-dependent fashion (Figure 6). A ~60% increase in GST activity was obtained in cells treated with 10 μM HNE (Figure 6(A)). Notably, the induction of NQO1 activity by HNE was more pronounced with a >2-fold induction of NQO1 activity observed at 10 μM HNE (Figure 6(B)). In line with the increased NQO1 activity, protein expression of NQO1 exhibited a similar concentration-dependent induction by HNE (Figure 6(C)). Incubation of H9c2 cells with 10 μM HNE also led to significant time-dependent induction of GSTA1 and NQO1 mRNA expression (Figure 7). The mRNA levels for both GSTA1 and NQO1 were increased by ~2–3-fold at 3–6 h; a remarkable 10–11-fold induction of GSTA1 mRNA and an 8–9-fold induction of NOQ1 mRNA were observed at 15–24 h (Figure 7).

Increased resistance of HNE-pretreated cells to H_2O_2- and SIN-induced cytotoxicity

Incubation of H9c2 cells with 50–125 μM H_2O_2 for 24 h led to decreases in cell viability as assessed by both MTT reduction and LDH release. Pretreatment of H9c2 cells with 10 μM HNE resulted in significant protection against H_2O_2-induced cytotoxicity (Figure 8(A),(B)). The intracellular ROS accumulation in HNE-pretreated cells after exposure to H_2O_2 was also significantly reduced as compared with that in control cells (Figure 8(C)). Moreover, the basal level of ROS in HNE-pretreated cells was also lower than that in control cells (Figure 8(C)), which was in line with the observation that HNE-pretreated cells had increased levels of antioxidants and phase 2 enzymes (Figures 2,4–7). Similar to what was observed with H_2O_2, HNE-pretreatment

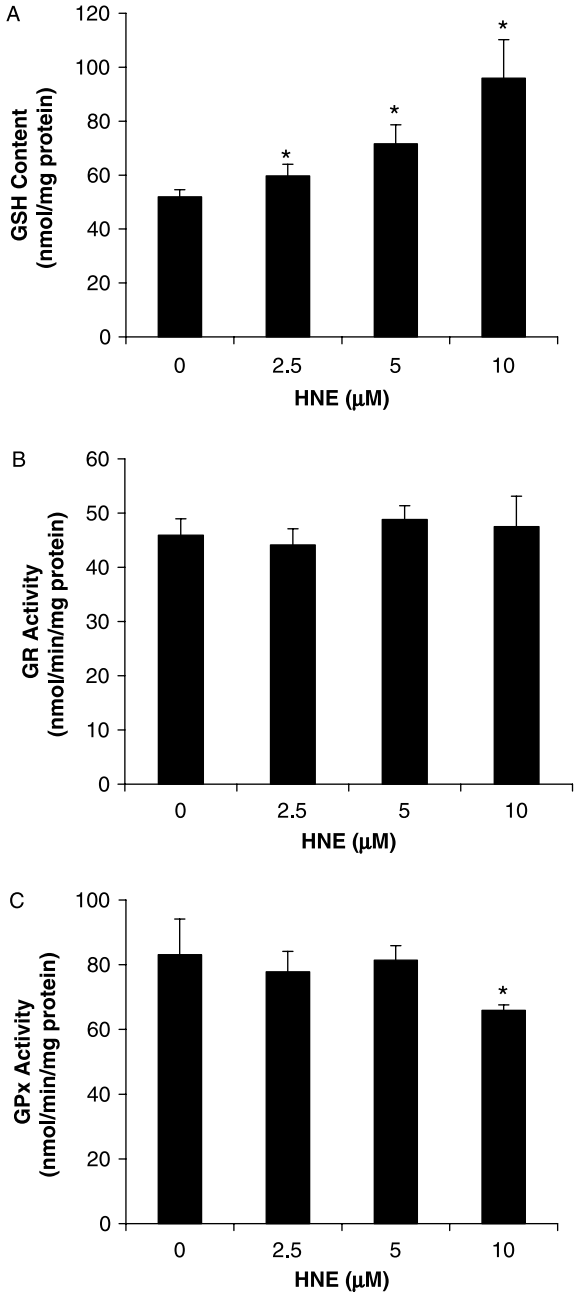

Figure 4. Effects of HNE treatment on GSH content (A), and GR (B) and GPx (C) activities in H9c2 cells. Cells were incubated with the indicated concentrations of HNE for 24 h, followed by measurement of GSH content, and GR and GPx activities. Values represent means ± SEM ($n = 4–6$). ⋆, Significantly different from "0 μM HNE" at $p < 0.05$.

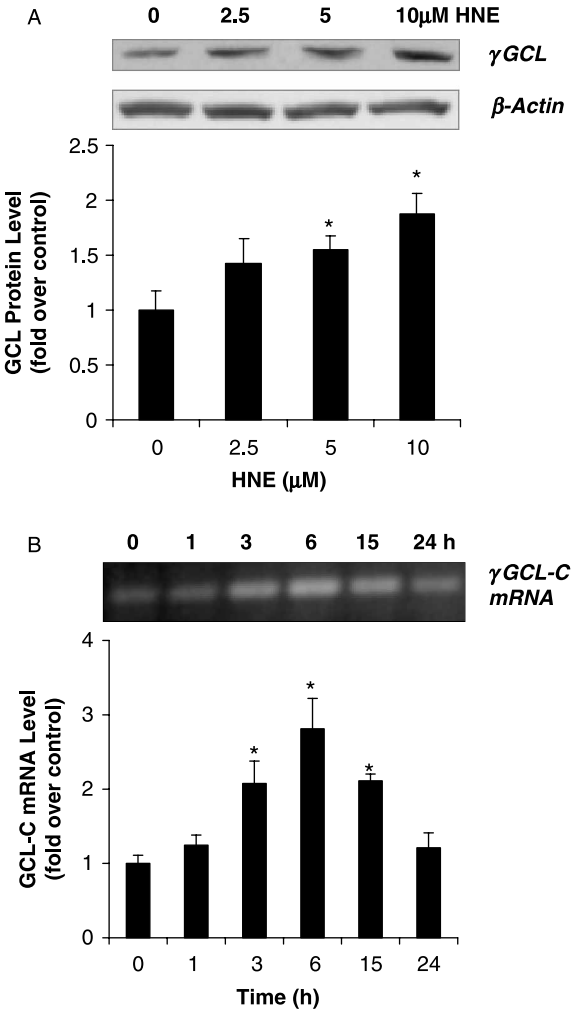

Figure 5. Expression of GCL protein (A) and GCL-C mRNA (B) in H9c2 cells treated with HNE. Cells were treated with the indicated concentrations of HNE for 24 h (A), or with 10 μM HNE for the indicated time points (B), followed by detection of GCL protein and GCL-C mRNA expression. In (A) or (B), top panel showing a representative gel picture of the GCL protein (A) or GCL-C mRNA (B) expression in H9c2 cells treated with HNE; low panel showing quantitative analysis of the GCL protein (A) or GCL-C mRNA (B) expression. Values represent means ± SEM ($n = 3$). ⋆, Significantly different from "0 μM HNE" (A) or 0 h (B) at $p < 0.05$. β-Action (A) serves as a loading control. In data not shown, HNE treatment did not affect the mRNA expression of β-actin.

of H9c2 cells also led to significant protection against the peroxynitrite-generator SIN-1-induced cytotoxicity as detected by both MTT reduction and release of LDH (Figure 9). Notably, the protection by HNE pretreatment was seen with all cytotoxic concentrations of SIN-1 used (Figure 9). The concentrations of H_2O_2 and SIN-1 used in this study are similar to those used in literature for investigation of oxidative cell injury.

Increased resistance of HNE-pretreated cells to cell injury induced by subsequent cytotoxic concentrations of HNE itself

To investigate if HNE-pretreated cells also became more resistant to high concentrations of HNE-induced cytotoxicity, 10 μM HNE-pretreated cells were exposed to cytotoxic concentrations of HNE (15–35 μM). As shown in Figure 10, HNE-pretreated cells showed increased resistance to cytotoxicity induced by high concentrations of HNE. Although the cytoprotective effects were observed at all HNE concentrations (15–35 μM) with regard to MTT

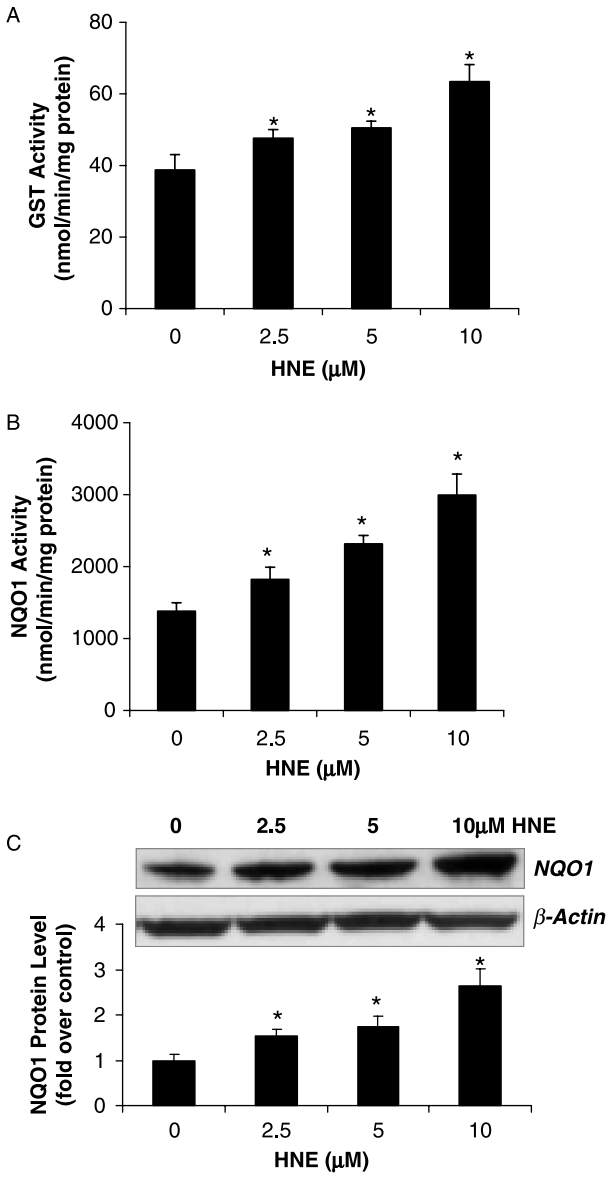

Figure 6. Effects of HNE on GST (A) and NQO1 (B) activities, and NOQ1 protein expression (C) in H9c2 cells. Cells were incubated with the indicated concentrations of HNE for 24 h, followed by determination of GST and NQO1 activities, and NQO1 protein expression. Values represent means ± SEM ($n = 4–5$ for (A) and (B); $n = 3$ for (C)). *, Significantly different from "0 μM HNE" at $p < 0.05$.

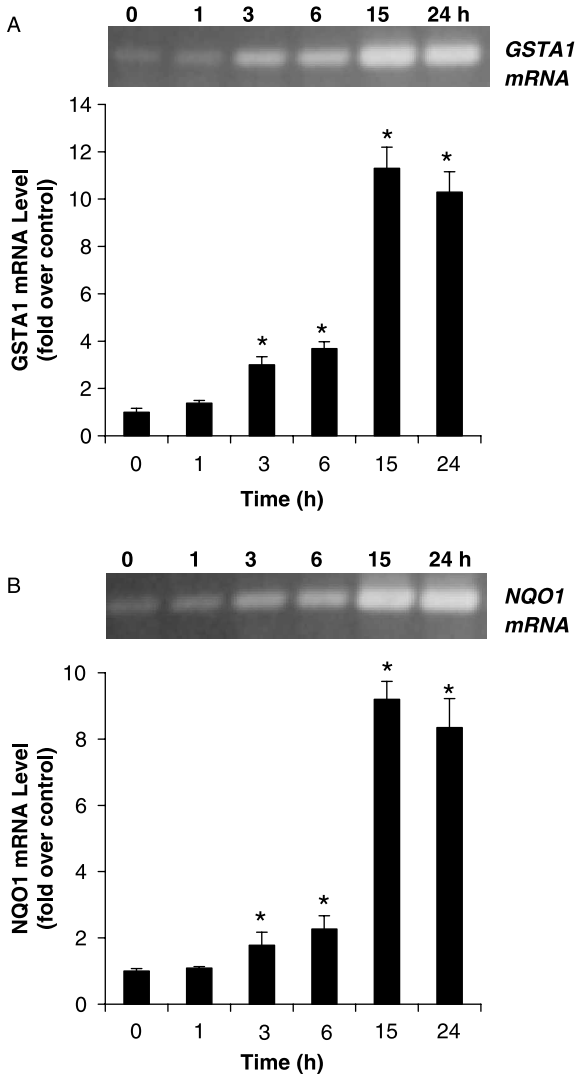

Figure 7. Time course of induction of mRNA expression of GSTA1 (A) and NQO1 (B) by HNE in H9c2 cells. In (A) or (B), top panel showing a representative gel picture of the mRNA expression at the indicated time points after treatment of H9c2 cells with 10 μM HNE; low panel showing quantitative analysis of the mRNA expression. Values represent means ± SEM ($n = 3$). *, Significantly different from 0 h at $p < 0.05$. In data not shown, HNE treatment did not affect the mRNA expression of β-actin.

reduction and LDH release, the protection against LDH release was more pronounced (Figure 10B).

Discussion

The implications of HNE in a wide variety of pathophysiological processes, including oxidative cardiovascular injury have led to extensive investigation of the mechanisms underling HNE-elicited toxicity as well as the cellular factors involved in its metabolism [1–8]. In this context, studies have shown that several enzymes, including GCL and GST that are involved in HNE detoxification, are induced by HNE itself at concentrations that do not elicit overt cytotoxicity [8,17]. However, it remains unclear if HNE is also capable of upregulating other antioxidants and phase 2 enzymes in cells. Moreover, the inducibility of antioxidants and phase 2 enzymes by HNE in cardiac cells, a target of HNE toxicity, had not been reported in literature. The results of this study demonstrated that incubation of rat myocardiac H9c2 cells with HNE at non-cytotoxic concentrations for 24 h led to significant induction of several antioxidants and phase 2 enzymes, including catalase, GSH/GCL, GST and NQO1. The induction of catalase and its mRNA expression by HNE in cells had not been previously reported. It remains unclear why catalase

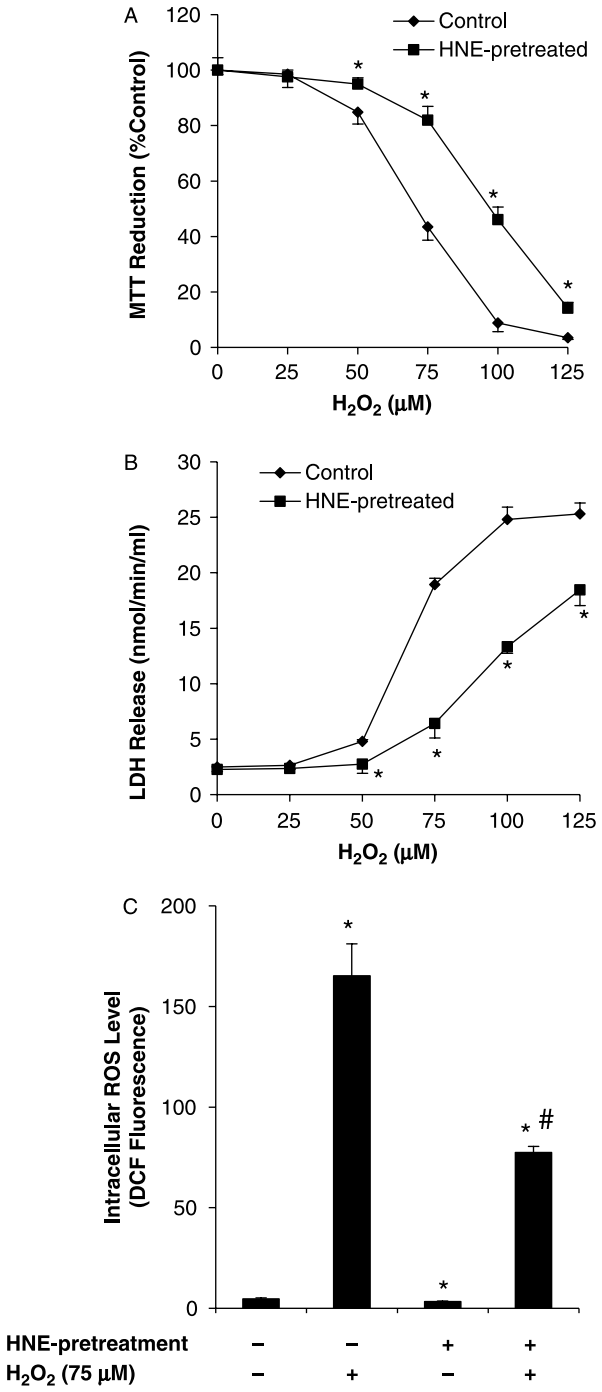

Figure 8. Inhibitory effects of HNE pretreatment on H_2O_2-mediated cytotoxicity (A and B) and intracellular ROS accumulation (C) in H9c2 cells. In (A) and (B), cells were incubated with or without 10 μM HNE for 24 h, followed by incubation with various concentrations of H_2O_2 for another 24 h. After this incubation, cell viability was determined by MTT reduction and LDH release. In (C), cells were incubated with or without 10 μM HNE for 24 h, followed by incubation with 10 μM DCFH-DA for 30 min. The intracellular ROS accumulation was determined by measuring the DCF-derived fluorescence after incubation of the cells with 75 μM H_2O_2 for another 30 min. Values represent means ± SEM ($n = 4$). In (A) and (B), ⋆, Significantly different from "0 μM H_2O_2" at $p < 0.05$. In (C), ⋆, Significantly different from control (No HNE-pretreatment, no H_2O_2); #, Significantly different from "control + H_2O_2" at $p < 0.05$.

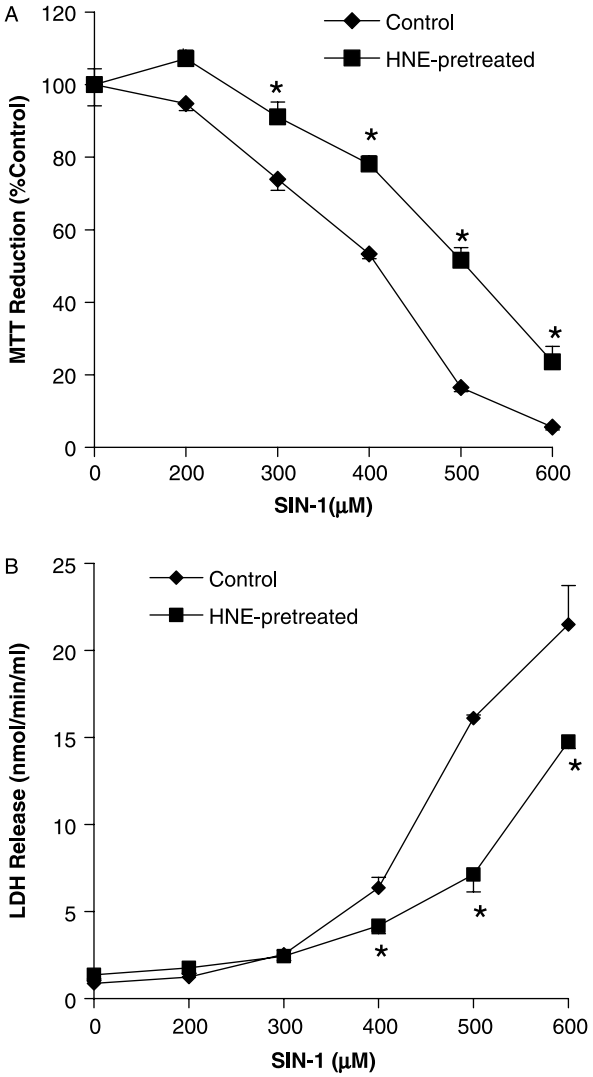

Figure 9. Protective effects of HNE pretreatment on SIN-1-induced cytotoxicity in H9c2 cells. Cells were incubated with or without 10 μM HNE for 24 h, followed by incubation with various concentrations of SIN-1 for another 24 h. After this incubation, cell viability was determined by MTT reduction and LDH release. Values represent means ± SEM ($n = 4$). ⋆, Significantly different from respective control at $p < 0.05$.

but not SOD was inducible by HNE in H9c2 cells. It was shown that HNE at concentrations similar to those used in this study could induce SOD in Jurkat T cells [18]. It thus appears that the inducibility of antioxidant enzymes by HNE varies with different types of cells employed.

Among the members of GSH system (GSH, GR and GPx), only GSH was shown to be inducible by HNE in H9c2 cells (Figure 4). The induction of GSH and GCL by HNE in H9c2 cells was consistent with previous observations made in other types of cells, where GSH/GCL was highly inducible by HNE [8]. The increased levels of GSH in HNE-treated H9c2 cells most likely resulted from the induction of the mRNA and protein expression of GCL, the key

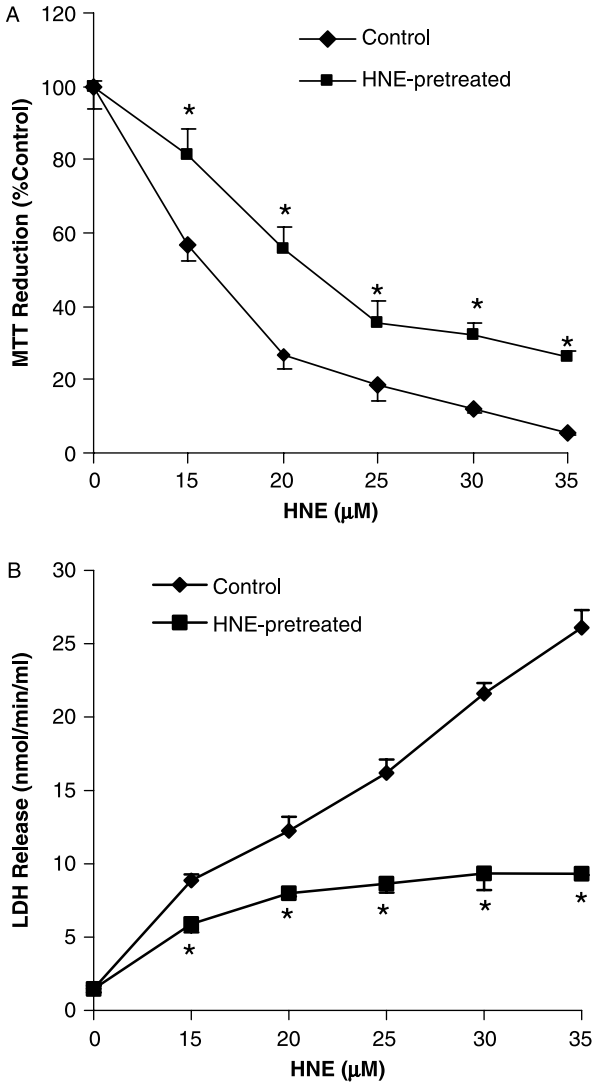

Figure 10. Protective effects of HNE pretreatment on cell injury induced by subsequent cytotoxic concentrations of HNE in H9c2 cells. Cells were incubated with or without 10 μM HNE for 24 h, followed by incubation with various cytotoxic concentrations of HNE for another 24 h. After this incubation, cell viability was determined by MTT reduction and LDH release. Values represent means + SEM ($n = 4$). *, Significantly different from respective control at $p < 0.05$.

enzyme involved in cellular GSH synthesis. A slight, but significant decrease in GPx activity was observed in H9c2 cells treated with 10 μM HNE (Figure 4(C)). Previously, it was reported that HNE could directly interact with GPx protein, leading to its inhibition in a cell-free system [19]. It remains unknown if this direct chemical-enzyme interaction is also responsible for the decreased GPx activity observed in the HNE-treated H9c2 cells. The remarkable induction of GSH/GCL in H9c2 cells by HNE was also in line with the concept that GSH is the principal detoxification factor for HNE in cells, including cardiomyocytes [5].

GST and NQO1 are two critical phase 2 enzymes involved in detoxification of electrophiles [20,21]. Recently, they have also been shown to participate in detoxification of ROS [20,21]. The induction of GST and NQO1 and their gene expression by HNE in cardiac cells had not been previously reported. It is known that GST exists as a family of multiple isozymes [20]. In this study, only GSTA1 mRNA expression was examined with regard to the inducibility by HNE in H9c2 cells. Further studies are needed to determine if other isoforms of GST are also inducible by HNE in cardiac cells.

HNE-pretreatment of H9c2 cells afforded significant protection against both H_2O_2 and SIN-1-induced cytotoxicity (Figures 8 and 9). SIN-1 autooxidizes at a physiological pH to produce equal moles of superoxide and nitric oxide, leading to the subsequent formation of peroxynitrite. As such SIN-1 is widely used to study the biological effects of peroxynitrite [10,14]. It is well-known that catalase and GSH/GPx are essential for H_2O_2 detoxification in mammalian cells. Recently, GSH/GPx has been identified as a critical pathway for peroxynitrite detoxification in cells [22]. Thus, induction of the above antioxidants by HNE in H9c2 cells would most likely account for the increased resistance of the NHE-pretreated cells to the above oxidant-induced cytotoxicity.

One important observation of this study was that upregulation of antioxidants and phase 2 enzymes by a non-cytotoxic concentration (10 μM) of HNE rendered the cells resistance to injury induced by subsequent exposure to HNE at higher, cytotoxic concentrations (Figure 10). Since HNE is primarily detoxified by GSH/GST [5–7], induction of the above 2 defense factors in H9c2 cells by 10 μM HNE pretreatment would apparently contribute to the cytoprotection against toxic concentrations of HNE. Such protective effects were much more pronounced when LDH release was used to determine the loss of cell viability, as compared with MTT reduction assay (Figure 10(B)). This might be due to that a decrease in MTT reduction could be indicative of either a decrease in cell viability (cell death) or an inhibition of mitochondrial function, or both [23]. In this context, HNE has been shown to potently inhibit mitochondrial activity [24], which might lead to the decreased reduction of MTT by mitochondria before the occurrence of cell death (release of LDH).

In summary, this study demonstrates that HNE at noncytotoxic concentrations is able to upregulate several key antioxidants and phase 2 enzymes in cardiac H9c2 cells, and that the increased cellular defenses are accompanied by significantly increased resistance to cytotoxicity elicited by ROS/RNS, as well as HNE itself. This adaptive cellular response might play a protective role in HNE- as well as ROS/RNS-induced pathogenesis during oxidative stress. In line with this conclusion, recently, Chen et al have elegantly demonstrated that HNE is capable of

inducing an adaptive response to oxidative stress in cultured cells, including neurons, which occurs via activation of the Nrf2 signaling pathway [25,26].

Acknowledgements

This work was supported in part by NIH grants CA91895 and HL71190 (Y. L.). J. L. Z. was supported by NIH grants HL63744, HL65608 and HL38324.

References

[1] Uchida K. 4-Hydroxy-2-nonenal: A product and mediator of oxidative stress. Prog Lipid Res 2003;42:318–343.
[2] Esterbauer H, Schaur RJ, Zollner H. Chemistry and biochemistry of 4-hydroxynonenal, malonaldehyde and related aldehydes. Free Radic Biol Med 1991;11:81–128.
[3] Strohmaier H, Hinghofer-Szalkay H, Schaur RJ. Detection of 4-hydroxynonenal (HNE) as a physiological component in human plasma. J Lipid Mediat Cell Signal 1995;11:51–61.
[4] Zarkovic N. 4-Hydroxynonenal as a bioactive marker of pathophysiological processes. Mol Aspects Med 2003;24: 281–291.
[5] Li Y, Cao Z, Zhu H, Trush MA. Differential roles of 3H-1,2-dithiole-3-thione-induced glutathione, glutathione S-transferase and aldose reductase in protecting against 4-hydroxy-2-nonenal toxicity in cultured cardiomyocytes. Arch Biochem Biophys 2005;439:80–90.
[6] Cao Z, Hardej D, Trombetta LD, Li Y. The Role of chemically-induced glutathione and glutathione S-transferase in protecting against 4-hydroxy-2-nonenal-mediated cytotoxicity in vascular smooth muscle cells. Cardiovasc Toxicol 2003;3:165–178.
[7] Petersen DR, Doorn JA. Reactions of 4-hydroxynonenal with proteins and cellular targets. Free Radic Biol Med 2004;37(7):937–945.
[8] Dickinson DA, Levonen AL, Moellering DR, Arnold EK, Zhang H, Darley-Usmar VM, Forman HJ. Human glutamate cysteine ligase gene regulation through the electrophile response element. Free Radic Biol Med 2004;37:1152–1159.
[9] Spitz DR, Oberley LW. An assay for superoxide dismutase activity in mammalian tissue homogenates. Anal Biochem 1989;179:8–18.
[10] Zhu H, Itoh K, Yamamoto M, Zweier JL, Li Y. Role of Nrf2 signaling in regulation of antioxidants and phase 2 enzymes in cardiac fibroblasts: Protection against reactive oxygen and nitrogen species-induced cell injury. FEBS Lett 2005;579:3029–3036.
[11] Aebi H. Catalase *in vitro*. Methods Enzymol 1984; 105:121–127.
[12] Wheeler CR, Salzman JA, Elsayed NM, Omaye ST, Korte DW. Automated assays for superoxide dismutase, catalase, glutathione peroxidase, and glutathione reductase activity. Anal Biochem 1990;184:193–199.
[13] Flohe L, Gunzler WA. Assays of glutathione peroxidase. Methods Enzymol 1984;105:114–119.
[14] Cao Z, Li Y. Protecting against peroxynitrite-mediated cytotoxicity in vascular smooth muscle cells via upregulating endogenous glutathione biosynthesis by 3H-1,2-dithiole-3-thione. Cardiovasc Toxicol 2004;4:339–353.
[15] Halford WP, Falco VC, Gebhardt BM, Carr DJ. The inherent quantitative capacity of the reverse transcription-polymerase chain reaction. Anal Biochem 1999;266:181–191.
[16] Cao Z, Li Y. Potent induction of cellular antioxidants and phase 2 enzymes by resveratrol in cardiomyocytes: Protection against oxidative and electrophilic injury. Eur J Pharmacol 2004;489:39–48.
[17] Yang Y, Cheng JZ, Singhal SS, Saini M, Pandya U, Awasthi S, Awasthi YC. Role of glutathione S-transferases in protection against lipid peroxidation: Overexpression of hGSTA2-2 in K562 cells protects against hydrogen peroxide-induced apoptosis and inhibits JNK and caspase 3 activation. J Biol Chem 2001;276:19220–19230.
[18] Larini A, Bianchi L, Bocci V. Effect of 4-hydroxynonenal on antioxidant capacity and apoptosis induction in Jurkat T cells. Free Radic Res 2004;38:509–516.
[19] Bosch-Morell F, Flohe L, Marin N, Romero FJ. 4-Hydroxynonenal inhibits glutathione peroxidase: Protection by glutathione. Free Radic Biol Med 1999;26:1383–1387.
[20] Hayes JD, Flanagan JU, Jowsey IR. Glutathione transferases. Annu Rev Pharmacol Toxicol 2005;45:51–88.
[21] Siegel D, Gustafson DL, Dehn DL, Han JY, Boonchoong P, Berliner LJ, Ross D. NAD(P)H:quinone oxidoreductase 1: Role as a superoxide scavenger. Mol Pharmacol 2004; 65:1238–1247.
[22] Sies H, Sharov VS, Klotz LO, Briviba K. Glutathione peroxidase protects against peroxynitrite-mediated oxidations: A new function for selenoproteins as peroxynitrite reductase. J Biol Chem 1997;272:27812–27817.
[23] Berridge MV, Herst PM, Tan AS. Tetrazolium dyes as tools in cell biology: New insights into their cellular reduction. Biotechnol Annu Rev 2005;11:127–152.
[24] Humphries KM, Yoo Y, Szweda LI. Inhibition of NADH-linked mitochondrial respiration by 4-hydroxy-2-nonenal. Biochemistry 1998;37:552–557.
[25] Chen ZH, Saito Y, Yoshida Y, Sekine A, Noguchi N, Niki E. 4-Hydroxynonenal induces adaptive response and enhances PC12 cell tolerance primarily through induction of thioredoxin reductase 1 via activation of Nrf2. J Biol Chem 2005;280:41921–41927.
[26] Chen ZH, Yoshida Y, Saito Y, Noguchi N, Niki E. Adaptive response induced by lipid peroxidation products in cell cultures. FEBS Lett 2006;580:479–483.